ELSEVIER

Dye-sensitized solar cells using a chlorophyll *a* derivative as the sensitizer and carotenoids having different conjugation lengths as redox spacers

Xiao-Feng Wang [a], Junfeng Xiang [a], Peng Wang [a], Yasushi Koyama [a,*],
Shozo Yanagida [b], Yuji Wada [c], Kazunori Hamada [d],
Shin-ichi Sasaki [d], Hitoshi Tamiaki [d]

[a] *Department of Chemistry, Faculty of Science and Technology, Kwansei Gakuin University, 2-1 Gakuen, Sanda, Hyogo 669-1337, Japan*
[b] *Innovation Center of Advanced Science, Osaka University, Suita, Osaka 565-0871, Japan*
[c] *Material and Life Science, Graduate School of Engineering, Osaka University, Suita, Osaka 565-0871, Japan*
[d] *Department of Bioscience and Biotechnology, Faculty of Science and Engineering, Ritsumeikan University, Kusatsu, Shiga 528-8577, Japan*

Abstract

Titania-based Grätzel-type solar cells were fabricated by the use of a chlorophyll *a* derivative (methyl 3-carboxy-3-devinyl-pyro-pheophorobide *a*) as the dye sensitizer. A 10% each of carotenoids, including neurosporene, spheroidene, lycopene, anhydrorhod-ovibrin and spirilloxanthin with numbers of conjugated double bonds, $n = 9$–13, was added as a conjugated spacer in order to neutralize the dye radical cation and to block the reverse electron transfer. The short-circuit current density (J_{sc}) and the solar energy-to-electricity conversion efficiency (η) systematically increased, with increasing n, from the values of 10.1 mA cm^{-2} and 3.1% (with no carotenoid) up to 11.5 mA cm^{-2} and 4.0% (with spirilloxanthin, $n = 13$), i.e., an enhancement of $\approx$30%.
© 2005 Elsevier B.V. All rights reserved.

1. Introduction

The photosynthetic systems have been refined during the history of photosynthetic organisms. Therefore, we believe that there is a chance to build a new type of dye-sensitized solar cells (DSSC) based on the principles and the materials of photosynthesis. However, chlorophyll *a* (Chl *a*) and pheophorbide *a*, for example, gave rise to very low photo-conversion efficiencies when incorporated into DSSC [1]. In the present investigation, we have prepared a Chl *a* derivative, in which the carboxyl group is directly attached to the conjugated macrocycle to facilitate efficient electron injection to TiO$_2$.

Carotenoids (Cars), photosynthetic pigments complementary to chlorophylls, play important roles in photosynthesis, which include not only the light-harvesting and photo-protective functions [2,3] but also the redox function [4]. β-Carotene in the reaction center of spinach photosystem II [5,6] as well as neurosporene, spheroidene and spheroidenone in the LH2 complexes of *Rhodobacter sphaeroides* [7] can become oxidized to form radical cations as a result of electron transfer, detailed mechanisms now being investigated [4]. The results indicate that carotenoids can potentially neutralize radical cation through electron transfer, when the conjugated systems are in close contact.
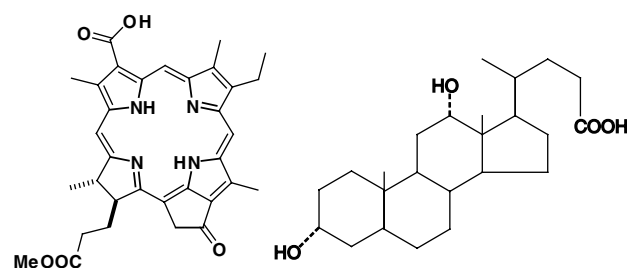
An idea underlying the present investigation is to use, as the dye sensitizer, such a derivative of chlorophyll *a*, and add a carotenoid (Car), as a conjugated spacer, in order to neutralize the dye radical cation and to block

* Corresponding author. Fax: +81 79 565 8408.
 *E-mail address:* ykoyama@kwansei.ac.jp (Y. Koyama).

the reverse electron transfer. This idea has not been tested yet as far as the authors know, although there have been some examples of photo-voltaic measurements and fabricating electrochemical cells (not as DSSCs) [8–10].

In the present investigation, we used, as the sensitizer, methyl 3-carboxy-3-devinyl-pyropheophorobide a (hereafter, abbreviated as PPB a der.), and added, as a conjugated spacer, a series of bacterial carotenoids, which includes neurosporene, spheroidene, lycopene, anhydrorhodovibrin and spirilloxanthin having the numbers of conjugated double bonds, $n = 9$–13, respectively. [Hereafter, they will be abbreviated as Neu, Sph, Lyc, Ahr, and Spx, respectively. See Scheme 1 for their chemical structures.] We used each Car in order to systematically tune the one-electron oxidation potential. We also tried deoxycholic acid (DCA), as a non-conjugated spacer for comparison, because the addition of stearic acid or lecithin enhanced the photocurrent generated by a Chl a monolayer-coated SnO_2 electrode [11,12].

Methyl 3-carboxy-3-devinyl-
pyropheophorbide a
(PPB a der.)

Deoxycholic acid
(DCA)

Neurosporene (Neu) n=9

Spheroidene (Sph) n=10

Lycopene (Lyc) n=11

Anhydrorhodovibrin (Ahr) n=12

Spirilloxanthin (Spx) n=13
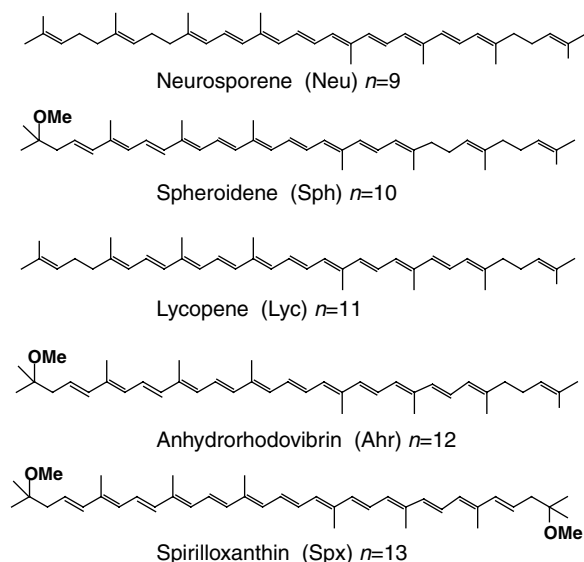
Scheme 1.

2. Experimental

PPB a der. was obtained by two steps of oxidation of the 3-vinyl group of methyl pyropheophorbide a [13–15]. Its structure was confirmed by ^{1}H NMR spectroscopy. Neu, Sph, Lyc, Ahr and Spx were isolated from *Rhodobacter sphaeroides* G1C, *Rhodobacter sphaeroides* 2.4.1, tomato juice, *Allochromatium vinosum* and *Rhodospirillum rubrum* S1, respectively, as described previously [16,17]. The purity of carotenoids was determined by HPLC (detection at the $1B_u^+$ absorption maximum) to be 99%, 100%, 99%, 99% and 97%, respectively.

Each dye-sensitized solar cells (DSSC) consisted of the optically transparent electrode (OTE), the counter electrode of Pt-sputtered, fluorine-doped tin oxide (FTO) glass (Nippon sheet Glass 10 Ω cm^{-2}), and a methoxyacetonitrile solution containing 0.1 M LiI, 0.05 M I_2 and 0.6 M 1,2-dimethyl-3-propyl-imidazolium iodide (DMPI). The OTE was fabricated by deposition of two layers of TiO_2 particles on an FTO glass; one layer (8-μm thick) consisted of 13-nm TiO_2 particles (Ti nanooxide T, Solarnix) for adsorbing the dye molecules, and the other (2-μm thick) consisted of 300-nm TiO_2 particles (CR-EL, Ishihara Sangyo) for scattering the incident light. Then, the TiO_2 deposited FTO glass was soaked overnight in THF solution, which contained the dye (PPB a der.) and one of the spacers (the above carotenoids and DCA) with a specified composition, to form the OTE.

The incident photon-to-current conversion efficiency (IPCE) profile of each DSSC was recorded under monochromatic irradiation (5 mW cm^{-2}) by the use of a setup for IPCE measurement (Bunko-Keiki PV-25 DYE), which consisted of a 300 W halogen lamp (Atago Bussan, XC-300), a monochromater (Instruments S. A. Triax 180) and a potentiostat (Hokuto Denko HA-151). The conversion efficiency (η) was determined under irradiation of AM 1.5 (100 mW cm^{-2}) light from a solar simulator (Yamashita Denso, YSS-80) equipped with a computer-controlled, voltage–current source meter (Advantest, R6246). To compare the effect of each carotenoid, at least four solar cells were fabricated, and their performance was averaged.

3. Results and discussion

3.1. Characterization of dye and spacer molecules

The structures of the dye and the spacer molecules can be characterized as follows (see Scheme 1): (1) PPB a der. consists of a conjugated macrocycle of chlorin skeleton and a carboxyl group directly attached to it. When the sensitizer is bound to the TiO_2 layer through the carboxylate group, π-electron in the conjugated system can be effectively injected into the TiO_2 nanoparticle. (2) DCA has been used as a non-conjugated

spacer to enhance the performance of DSSCs [1]. It is supposed to prevent the aggregation of dye sensitizer molecules, and as a result, the annihilation of singlet and triplet excitations. In the present system, the planar PPB a der. tends to be bound to the TiO_2 layer through the carboxylate group to form a large aggregate in a card-packed manner. DCA can also be bound to the TiO_2 layer through the carboxylate group, intervening the stacking of the dye sensitizer. (3) A set of bacterial Cars includes Neu, Sph, Lyc, Ahr and Spx having the number of conjugated double bonds, $n = 9$–13, respectively, whose peripheral structures are different from one another. Although those molecules have no carboxyl group, they can intervene the stacking of the dye molecules through the dispersive interaction between the linear and the planar conjugated systems of the Car and PPB a der. molecules (vide infra). Therefore, each Car is supposed to function as a conjugated spacer having the redox function.

3.2. Energies and one-electron oxidation potentials of the dye and Car molecules: possible mechanisms of enhancement of photocurrent by Cars

3.2.1. Energy-transfer mechanism

As mentioned in Section 1, Cars have the light-harvesting function; actually, there was a proposal that energy transfer from a carotenoid, canthaxanthin, to chlorophyll a enhanced the photocurrent generated by the latter [8].

Fig. 1 shows an energy diagram for the low-lying singlet states of the present set of Cars in the crystalline state determined by the measurement of resonance-Raman

Fig. 1. Energies of the $1B_u^+$, $1B_u^-$ and $2A_g^-$ states of Cars as linear functions of $1/(2n + 1)$ [15]. The Q_x and Q_y levels of PPB a der. in THF solution and those of BChl a in the LH2 antenna-complex [17,18] are also shown for comparison.

excitation profiles [16]. In the present case of PPB a der., the Q_x and Q_y levels are substantially shifted to the higher energies in comparison to those of bacteriochlorophylls (BChls) in the LH2 and LH1 complexes, in which the $1B_u^+ \rightarrow Q_x$, $1B_u^- \rightarrow Q_x$ and $2A_g^- \rightarrow Q_y$ singlet energy-transfer reactions take place in Cars with $n = 9$ and 10, whereas only the $1B_u^+ \rightarrow Q_x$ energy transfer takes place in Cars with $n = 11$–13, in competition with the rapid internal conversion of $1B_u^+ \rightarrow 1B_u^- \rightarrow 2A_g^- \rightarrow$ ground [18,19] (see those references for the definition and the roles of the singlet states of Cars and BChls). Judging from the relative energy levels of Cars and PPB a der., all the $1B_u^+$, $1B_u^-$ and $2A_g^-$ channels are open only in Neu ($n = 9$), and therefore, there can be efficient singlet-energy transfer to PPB a der. Most importantly, no singlet-energy transfer should occur for Spx ($n = 13$) having the longest conjugated chain.

3.2.2. Electron-transfer mechanism

Another possible mechanism originates from the redox function of Cars, i.e., electron transfer to the dye radical cation, mentioned in Section 1 as 'the idea underlying the present investigation'. More specifically, when the dye sensitizer, i.e., PPB a der., is excited to the Q_y state by absorption of photon, electron can be injected to TiO_2 to generate the charge-separated state consisting of the dye radical cation and electron on TiO_2. However, the reverse electron transfer to cause charge recombination can always take place, which is the major reason for the reduction of the photocurrent. When the neighboring Car molecule transfers its electron to neutralize the dye radical cation, another charge-separated state can be generated between the Car radical cation and the electron on TiO_2. Importantly, this charge-separated state is expected to be much more stable, because no direct pathways for the reverse electron transfer are available.

Table 1 lists the values of one-electron oxidation potentials of PPB a der. and the set of Cars. The one-electron oxidation potentials of all the Cars are on the negative side of that of PPB a der., a fact which indicates that an electron can be transferred from the former to the latter. Each Car radical cation can be re-reduced and stabilized by the redox couple I^-/I_3^-, having the one-electron oxidation potential of ≈ 0.4 V vs. NHE. In particular, Spx ($n = 13$) showing the one-electron oxidation potential of 0.77 must have the highest potential to be oxidized, and therefore, exhibit the highest enhancement of photocurrent. This expectation contrasts to that in 'the energy-transfer mechanism' mentioned above.
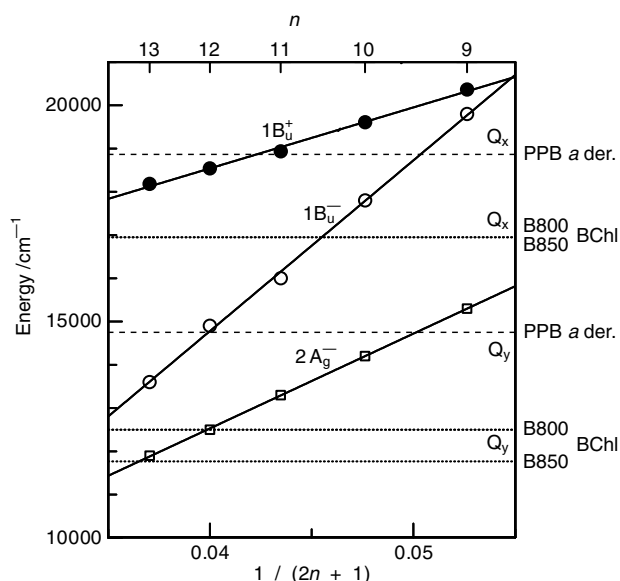
Table 1
One-electron oxidation potentials (vs. NHE in eV) of PPB a der. and Cars

PPB a der. alone	Car				
	Neu	Sph	Lyc	Ahr	Spx
1.16	0.83	0.81	0.79	0.78	0.77

Further, the generation of Car radical cation was confirmed, by means of subpicosecond time-resolved absorption spectroscopy, when PPB a der. was bound to TiO_2 nanoparticles in suspension, and then, each Car was added (J. Xiang, X. Wang, Y. Kakitani, Y. Koyama, S. Sasaki and H. Tamiaki, unpublished results). The peaks appearing in the time-resolved spectra were assigned to PPB a der.$^{·+}$ and each Car$^{·+}$ based on spectral comparison with those generated electrochemically free in solution. The PPB a der.$^{·+}$ peak appeared within 0.2 ps, and decayed slowly at least until 1 ns. On the other hand, the Car$^{·+}$ peak increased in intensity in accord with the decay of the PPB a der.$^{·+}$. The results supported the idea that the initial electron injection from PPB a der. to TiO_2 is rapidly followed by electron transfer from Car to PPB a der.$^{·+}$.

3.3. The effect of Cars on the performance of DSSC: dependence on their conjugation length

Fig. 2 shows the IPCE profiles and the I–V curves, when 10% of each Car having different n was added;
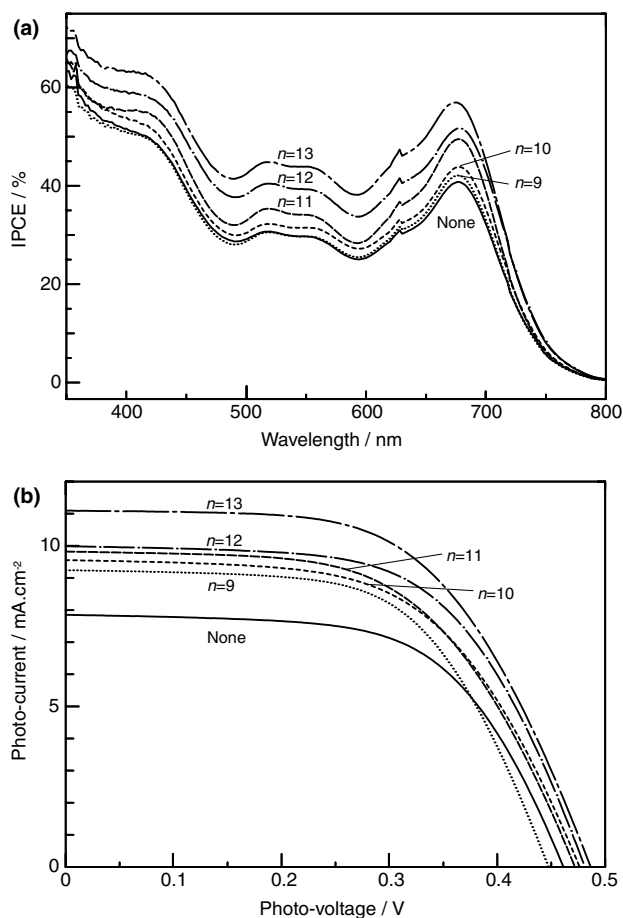
those recorded for the PPB a der.-sensitized solar cell without Cars are also shown for comparison. The intensity of the IPCE profile as well as the photocurrent density in the I–V curve increases in the order, none $< n = 9 < n = 10 < n = 11 < n = 12 < n = 13$. Table 2 lists the values relevant to the performance of DSSC obtained from the data (see Supporting Materials). Fig. 3 clearly shows that both the $IPCE_{676}$ and the η values increase as linear functions of n, within experimental error, an observation which is in agreement with the prediction based on 'the electron-transfer mechanism' described in Section 3.2.2. Spx having the most negative one-electron oxidation potential gives rise to the highest IPCE value and the highest conversion efficiency, η.

3.3.1. Effects of dilution of the dye sensitizer with non-conjugated and conjugated spacers

Fig. 4a,c shows the effects of dilution of PPB a der. with DCA (a non-conjugated spacer) and Spx (the most effective conjugated spacer) on the IPCE profile; the concentrations of PPB a der. remaining on the TiO_2 layer are indicated in this figure. The relevant parameters, obtained from the measurements of the IPCE profiles and the I–V curves for the two spacers, are listed in
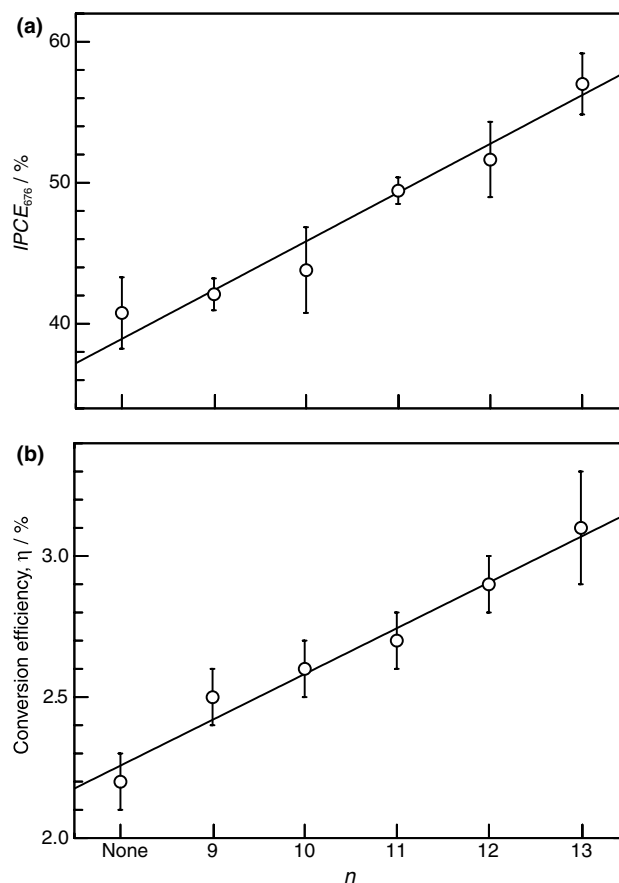

Fig. 2. The IPCE profiles (a) and the I–V curves (b) for the PPB a der.-sensitized solar cell without Car and with a 10% each of Cars having $n = 9$–13.

Fig. 3. The $IPCE_{676}$ (a) and the conversion efficiency η (b) as linear functions of n, when a 10% each of Cars was added.
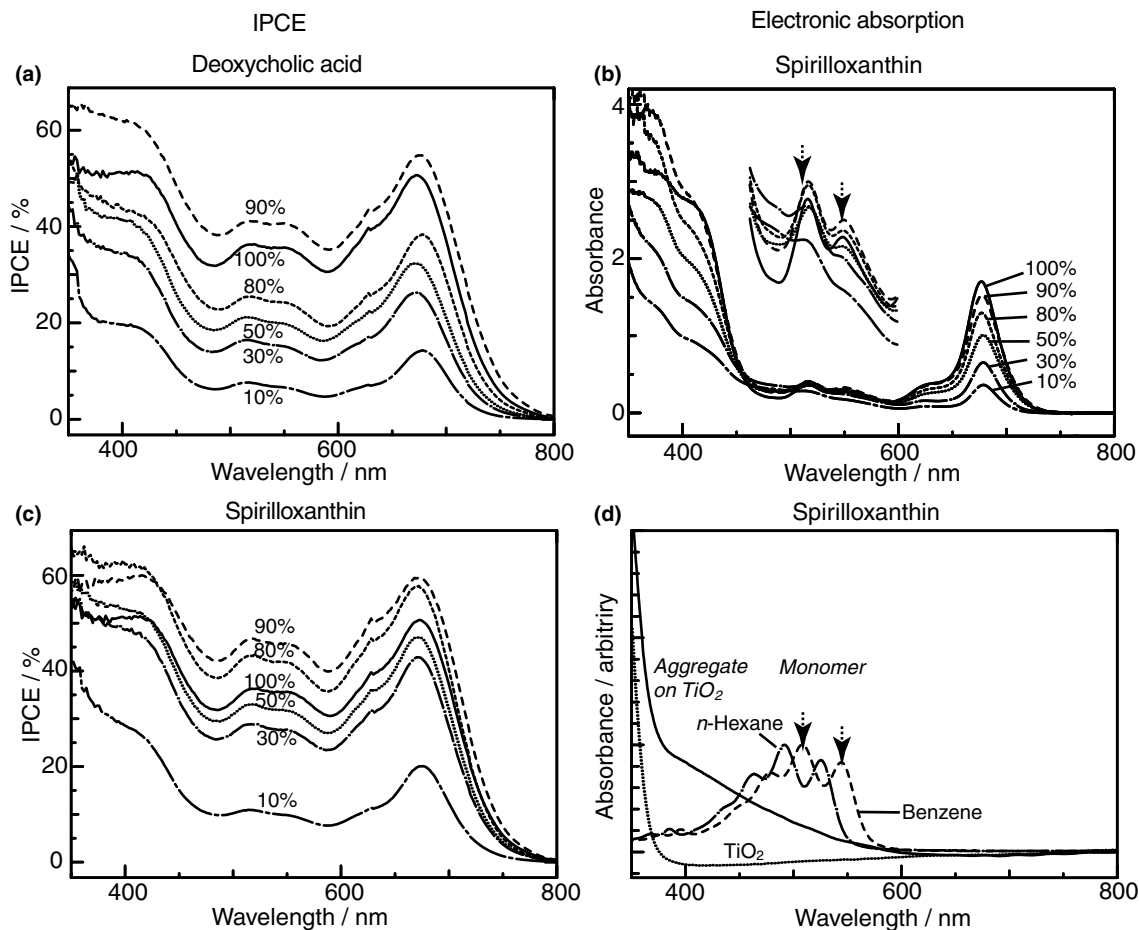
Fig. 4. Effects of dilution of PPB *a* der. with DCA and Spx on the IPCE profile (a,c), and the effects of dilution on the electronic absorption spectra (b). The concentrations of PPB *a* der. remaining on the TiO$_2$ layer are indicated in %. The absorption spectra of Spx in *n*-hexane and benzene solutions, and bound to the TiO$_2$ layer (d) are also shown for comparison.

Table 3 (see Supporting Materials). [The dye sensitizer had been diluted with each spacer in the THF solution, into which the TiO$_2$ layer was soaked overnight. We assumed here that the dye and the spacer molecules were deposited keeping the relative composition.]

Fig. 5 depicts the concentration dependence of the IPCE value at the Q$_y$ peak for DCA and Spx. The profiles of concentration dependence in the non-conjugated and conjugated spacers are analogous to each other, suggesting that basic mechanisms of the dilution effect include something in common. This figure also exhibits a definitive difference between the two spacers: The conjugated spacer always exhibits a higher IPCE value than the non-conjugated spacer. This observation indicates that there is some additional effect in the conjugated spacer. The difference between the conjugated and non-conjugated spacers appears more clearly, when the amount of each spacer is comparable to that of PPB *a* der. Both results support 'the electron-transfer mechanism' mentioned in Section 3.2.2.

Fig. 4b,d shows the effect of dilution of PPB *a* der. with Spx on the absorption spectra of those pigments
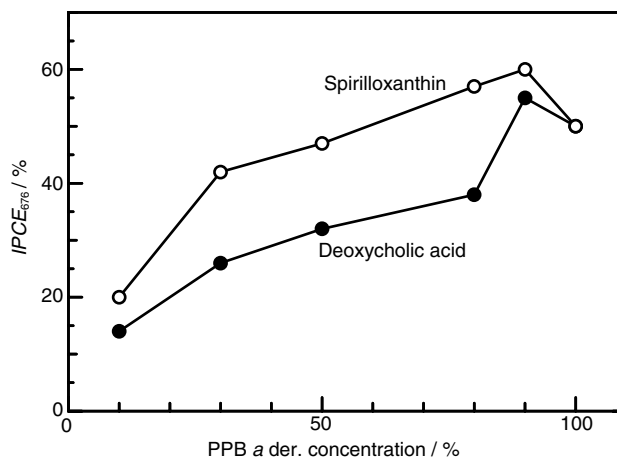

Fig. 5. Concentration dependence of the IPCE values at the Q$_y$ peak for the non-conjugated and conjugated spacers, i.e., DCA and Spx.

deposited on the TiO$_2$ layer, and the absorption spectra of monomeric Spx in solution and aggregated Spx deposited on the TiO$_2$ film. When diluted, the Q$_y$ absorption of PPB *a* der. becomes systematically

weakened, but the spectral changes of the Car are less clear. At the initial dilution, however, the expansion of the ordinate scale in the 400–600 nm region exhibits the enhancement of the pair of peaks, which roughly corresponds, in wavelength, to that of the Car not in *n*-hexane but in benzene solution. This observation suggests that the monomeric Car molecules are placed between the PPB *a* der. molecules under the influence of dispersive interaction with the macrocycle of PPB *a* der. At the later stage of dilution, the set of the spectra exhibits a contribution of inclined spectrum, originating from the Car aggregate formed on the TiO$_2$ layer.

Acknowledgments

Appendix A. Supplementary data

Supplementary data associated with this article can be found, in the online version, at doi:10.1016/j.cplett.2005.04.067.

References

[1] A. Kay, M. Grätzel, J. Phys. Chem. 97 (1993) 6272.

[2] H.A. Frank, R.J. Cogdell, in: A. Young, G. Britton (Eds.), Carotenoids in Photosynthesis, Chapman & Hall, London, 1993, p. 252.

[3] Y. Koyama, R. Fujii, in: H.A. Frank, A.J. Young, G. Britton, R.J. Cogdell (Eds.), Advances in Photosynthesis, The Photochemistry of Carotenoids, vol. 8, Kluwer Academic Publishers, Dordrecht, 1999, p. 161.

[4] H.A. Frank, G.W. Brudvig, Biochemistry 43 (2004) 8607.

[5] T. Noguchi, T. Mitsuka, Y. Inoue, FEBS Lett. 356 (1994) 179.

[6] J. Hanley, Y. Deligiannakis, A. Pascal, P. Faller, A.W. Rutherford, Biochemistry 38 (1999) 8189.

[7] T. Polívka, D. Zigmantas, J.L. Herek, Z. He, T. Pascher, T. Pullerits, R.J. Cogdell, H.A. Frank, V. Sundström, J. Phys. Chem. B 106 (2002) 11016.

[8] A. Diarra, S. Hotchandani, J.-J. Max, R.M. Leblanc, Chem. Soc., Faraday Trans. 2 82 (1986) 2217.

[9] M.L. Curri, A. Petrella, M. Striccoli, P.D. Cozzoli, P. Cosma, A. Agostiano, Synth. Met. 139 (2003) 593.

[10] A. Petrella, P.D. Cozzoli, M.L. Curri, M. Striccoli, P. Cosma, A. Agostiano, Bioelectrochemistry 63 (2004) 99.

[11] T. Miyasaka, T. Watanabe, A. Fujishima, K. Honda, J. Am. Chem. Soc. 100 (1978) 6657.

[12] T. Miyasaka, T. Watanabe, A. Fujishima, K. Honda, Nature 277 (1979) 638.

[13] H. Tamiaki, M. Amakawa, Y. Shimono, R. Tanikaga, A.R. Holzwarth, K. Schaffner, Photochem. Photobiol. 63 (1996) 92.

[14] H. Tamiaki, S. Miyata, Y. Kureishi, R. Tanikaga, Tetrahedron 52 (1996) 12421.

[15] A. Osuka, Y. Wada, S. Shinoda, Tetrahedron 52 (1996) 4311.

[16] K. Furuichi, T. Sashima, Y. Koyama, Chem. Phys. Lett. 356 (2002) 547.

[17] R. Fujii, T. Inaba, Y. Watanabe, Y. Koyama, J.-P. Zhang, Chem. Phys. Lett. 369 (2003) 165.

[18] F.S. Rondonuwu, K. Yokoyama, R. Fujii, Y. Koyama, R.J. Cogdell, Y. Watanabe, Chem. Phys. Lett. 390 (2004) 314.

[19] J. Akahane, F.S. Rondonuwu, L. Fieder, Y. Watanabe, Y. Koyama, Chem. Phys. Lett. 393 (2004) 184.